$mPEG_{2000}$-DSPE	1,2-Distearoyl-sn-glycero-3-phosphoethanolamine-*n*-[methoxy (polyethyleneglycol)-2000]
PBS	Phosphate-buffered saline
PEG	Polyethylene glycol
POPC	1-Palmitoyl-2-oleoylphosphatidylcholine
TE buffer	Tris-EDTA buffer
5-FU	5-Fluorouracil
^{3}H-CHE	Tritium-cholesterylhexadecyl ether

Introduction

Small interfering RNAs (siRNAs) are short double-stranded RNAs which induce a sequence-specific and potent gene silencing effect by means of RNA interference (RNAi) [1]. siRNA can inhibit the expression of the targeted gene, and therefore siRNAs are not only promising biological tools but also represent novel medicines against a variety of gene-mediated diseases including cancer [2, 3]. Despite the proven efficacy of siRNA, thus far only limited RNAi effects have been achieved in vivo following systemic injection, mainly due to rapid enzymatic degradation and poor cellular uptake [4, 5]. Therefore, novel delivery systems which protect siRNA against enzymatic degradation and permit high accessibility to and uptake by target cells are indispensably requested.

Several studies confirmed that systemic delivery of siRNA to solid tumors as well as cancer metastasis is greatly improved when the siRNA is associated with nanocarrier systems such as liposomes, lipid- or polymer-based nanoparticles [6–8]. However, efficient systemic delivery of siRNA-lipoplexes to tumor tissue is still hampered by several barriers such as irregular vasculature, variable permeability of blood vessels and high interstitial fluid pressure of solid tumors. Consequently, observed therapeutic efficacies of nanocarrier-encapsulated siRNA are still rather poor.

Metronomic chemotherapy, which refers to the frequent repeated administration of chemotherapeutics at doses significantly below the maximum tolerated dose without prolonged drug-free breaks, is a novel approach to control advanced cancer [9, 10]. Drugs that can be administered orally, such as cyclophosphamide (CPA) [11], etoposide [12], capecitabine [13], UFT [14], and S-1 (an oral formulation of 5-fluorouracil (5-FU) prodrug) [15, 16], would meet the requirements of prolonged daily administration schedules. We recently showed that metronomic CPA dosing enhanced the intratumoral accumulation of co-administered doxorubicin-containing polyethylene glycol (PEG)-coated liposomes, and consequently, this combination therapy exerted an excellent antitumor activity in a murine tumor model without severe overlapping side-effects [17, 18]. S-1 metronomic dosing also enhanced the accumulation and distribution of both PEG-coated liposomes containing oxaliplatin [19] and PEG-coated siBcl-2-lipoplexes in solid tumor, resulting in a potent tumor growth suppressive effects [20]. These observations led us to assume that the combination with metronomic S-1 dosing improves the tumor accumulation and distribution of PEG-coated siRNA-lipoplexes, by virtue of circumventing the above-mentioned obstacles, thereby enhancing the antitumor effect of siRNA, as compared to monotherapy with either S-1 or PEG-coated siRNA-lipoplexes alone.

In this study, to extend our work, we further investigated the effect of metronomic S-1 dosing on the intratumoral accumulation and distribution of PEG-coated siAgo2-lipoplexes both quantitatively and qualitatively in a Lewis lung carcinoma cells (LLCC) murine solid tumor model. In addition, the antitumor effect of this combination therapy was investigated.

Materials and methods

Materials

S-1 [consisting of tegafur (a prodrug of 5-FU)/5-chloro-2,4-dihydroxypyrimidine (an inhibitor of 5-FU catabolism)/potassium oxonate (a reducer of gastrointestinal toxicity) in a molar ratio 1/0.4/1] was generously donated by Taiho Pharmaceutical Co. Ltd (Tokyo, Japan). 1-Palmitoyl-2-oleoylphosphatidylcholine (POPC), dioleoylphosphatidylethanolamine (DOPE), and 1,2-distearoyl-*sn*-glycero-3-phosphoethanolamine-*n*-[methoxy(polyethylene glycol)-2000] ($mPEG_{2000}$-DSPE) were generously donated by NOF (Tokyo, Japan). Cholesterol (CHOL) was purchased from Wako Pure Chemical Co. Ltd (Osaka, Japan). A cationic lipid, O,O′-ditetradecanoyl-N-(alpha-trimethyl ammonio acetyl) diethanolamine chloride (DC-6-14) was purchased from Sogo Pharmaceutical Co. Ltd (Tokyo, Japan). The hydrophobic fluorescent dyes, 1,1′-dioctadecyl-3,3,3′,3′-tetramethyl-indodicarbocyanine perchlorate (DiD) and 1,1′-dioctadecyl-3, 3, 3′, 3′-tetramethyl-indocarbocyanine perchlorate (DiI), were purchased from Invitrogen (San Diego, CA, USA). ^{3}H-cholesterylhexadecyl ether (^{3}H-CHE) was purchased from Perkin-Elmer Japan (Yokohama, Japan). All other reagents were of analytical grade.

Animals and tumor cell line

Five-week-old male C57BL/6 mice were purchased from Japan SLC (Shizuoka, Japan). The experimental animals were allowed free access to water and conventional mouse chow (not folic acid-deficient diet), and were housed under controlled environmental conditions (constant temperature,

humidity, and 12-h dark–light cycle). All animal experiments were evaluated and approved by the Animal and Ethics Review Committee of the University of Tokushima. LLCC was purchased from Cell Resource Center for Biomedical Research (Institute of Development, Aging and Cancer, Tohoku University). The cells were maintained in Dulbecco's modified Eagle's medium (DMEM) (Nissui Pharmaceutical Co. Ltd, Tokyo, Japan) supplemented with 10% heat-inactivated fetal bovine serum (Japan Bioserum, Hiroshima, Japan), 10 mM L-glutamine, 100 U/ml penicillin, and 100 μg/ml streptomycin in a 5% CO_2/air incubator at 37°C.

siRNA

All siRNAs, chemically synthesized and purified by HPLC, were purchased from Nippon EGT (Toyama, Japan). The sequence of siRNA against Argonaute2 (siAgo2) was sense: 5′-UGA GGC ACU UAC CAU CCA UTT-3′ and antisense sequence, 5′-AUG GAU GGU AAG UGC CUC ATT-3′ [21]. The sequence of the non-silencing control siRNA (siNS), which was targeting against GFP, was sense: 5′-GGC UAC GUC CAG GAG CGC ATT-3′ and antisense: 5′-UGC GCU CCU GGA CGU AGC CTT-3′ [22].

For the preparation of siRNA duplexes, the complementary antisense and sense strands in TE buffer [10 μM Tris–HCl, 1 μM EDTA (pH 8.0), DNase and RNase free grade, (Nippon Gene, Tokyo, Japan)] were mixed in equal amounts, followed by heating at 90°C for 1 min. The reaction mixture was then allowed to cool at room temperature. The quality of siRNA duplexes was checked by 15% PAGE. The final concentration of the duplexes was 50 μM in TE buffer.

Preparation of cationic liposomes

Cationic liposomes composed of DOPE/POPC/CHOL/DC-6-14 (3:2:3:2, molar ratio) were prepared as described previously [23]. Briefly, the lipids were dissolved in chloroform, and after evaporation of the organic solvent, the resulting thin lipid film was hydrated with 9% sucrose to produce multilamellar vesicles (MLVs). The MLVs were sized by repeated extrusion through polycarbonate membrane filters (Nuclepore, Pleasanton, CA, USA) with consecutive pore sizes of 400, 200, and 100 nm. The mean diameters and zeta potentials of the resulting liposomes were determined using a NICOMP 370 HPL submicron particle analyzer (Particle Sizing System, Goleta, CA, USA). The mean diameter and zeta potential for cationic liposomes were 106.4±1.6 nm and 26.5±1.1 mV (n=3), respectively. The concentration of phospholipids was determined by colorimetric assay [24].

Preparation of PEG-coated siRNA-lipoplexes

For the preparation of siRNA/cationic liposome complexes (siRNA-lipoplexes), siRNAs, and cationic liposomes were mixed at a charge ratio of 3.81 (+/−), which was equal to 800:1 (lipid/siRNA, molar ratio), and the mixture was vigorously vortexed (3,200 rpm, 10 min, room temperature) to form siRNA-lipoplexes. The mean diameter and zeta potential of siRNA-lipoplexes were 398.6±42.0 nm and 19.6± 1.1 mV (n=3), respectively. For in vivo application, siRNA-lipoplexes were surface-modified by polyethylene glycol (PEG)-conjugated lipid (PEGylation) using a post-insertion technique [25]. Briefly, $mPEG_{2000}$-DSPE (5 mol% of total lipid) in 9% sucrose solution was added to the siRNA-lipoplex solution, and the mixture was gently shaken for 1 h at 37°C. The mean diameter and zeta potential of PEG-coated siRNA-lipoplexes were 406.3±27.4 nm and 15.8± 2.0 mV (n=3), respectively. To detect the free siRNA in the prepared PEG-coated siRNA-lipoplex, electrophoresis was performed on 2% agarose gel in 40 mM Tris–acetate/1 mM EDTA buffer and siRNA visualization is carried out using a UV transilluminator. No bands relating free siRNA were detected, indicating that virtually 100% of the siRNA was associated with and/or encapsulated in the PEG-coated siRNA-lipoplexes. To follow the biodistribution of PEG-coated siRNA-lipoplexes, they were labeled with a trace amount of ^{3}H-CHE (40 μCi/μmol lipid) as a non-exchangeable lipid phase marker. For in vivo imaging experiments, the lipoplexes were labeled with 1 mol% of the hydrophobic fluorescent dye DiD. For the intratumoral distribution study, liposomes were labeled with 1 mol% of the hydrophobic fluorescence dye DiI.

In vivo fluorescence imaging of PEG-coated siRNA-lipoplexes

LLCC (2×10^6) were inoculated subcutaneously in the back region of the mice. From day 6 after LLCC inoculation, mice were daily treated orally with S-1 at a metronomic dosing schedule for 7 days (6.9 mg tegafur/kg). On the last day of S-1 treatment, mice were injected intravenously with DiD-labeled PEG-coated siRNA-lipoplexes [25 mg total lipid and 0.83 mg siRNA (siNS)/kg]. At 24 h post-injection, mice were anesthetized with isoflurane (FORANE, Abott Japan, Osaka, Japan), a short-acting anesthetic, and maintained throughout the imaging process on a heating pad at 37°C. Fluorescence imaging was performed with a fluorescence image analyzer LAS-4000IR (Fujifilm, Tokyo, Japan). The fluorescence images were acquired with a 1/15-s exposure time and the images were visualized using 644-nm excitation and 665-nm emission filter sets.

Biodistribution study of PEG-coated siRNA-lipoplexes in tumor-bearing mice

To assess the tissue distribution of PEG-coated siRNA-lipoplexes, tumor-bearing mice pretreated with metronomic S-1 dosing [6.9 mg tegafur/kg] for either 4 or 7 days were injected intravenously with ^{3}H-CHE-labeled PEG-coated siRNA-lipoplexes [25 mg lipid/kg mouse and 0.83 mg siRNA (siNS)/kg]. At 24 h post-injection, mice were anesthetized, and blood (100 μl) was withdrawn by heart puncture. After withdrawing the blood samples, mice were sacrificed and liver, spleen, lung, kidney, and tumor were collected. Tissue samples were washed with cold phosphate-buffered saline (PBS, 37 mM NaCl, 2.7 mM KCl, 8.1 mM Na_2HPO_4 and 1.47 mM KH_2PO_4; pH 7.4) and weighed after removing excess fluid. Radioactivity in blood and tissue samples was assayed as described previously [26].

Intratumoral distribution of PEG-coated siRNA-lipoplexes

To evaluate the effect of metronomic S-1 dosing (tegafur 6.9 mg/kg) on the intratumoral distribution of PEG-coated siRNA-lipoplexes, DiI-labeled lipoplexes [25 mg lipid/kg mouse and 0.83 mg siRNA (siNS)/kg] were intravenously injected to LLCC-bearing mice pretreated orally with metronomic S-1 for 7 days. At 24 h post-injection, mice were sacrificed. Then, tumors were harvested and snap frozen in OTC compound (Sakura Fintechnical, Tokyo, Japan) by dry-iced acetone. Sections of frozen samples (6 μm thick, five sections/one tumor block) were examined using a BZ-9000 fluorescence microscope (Keyence, Osaka, Japan). All obtained images from one section were joined and were considered as the image of the entire tumor section. The fluorescence intensity of the images was determined by using the measurement-module software (BZ-H1M, Keyence). In some experiments, to visualize tumor vasculature, FITC-conjugated rat anti-mouse CD31 monoclonal antibody (20 μg/head) (Millipore, Billerica, MA, USA) was intravenously injected 10 min before sacrifice.

Antitumor effect of combination treatment

On day 6 after tumor inoculation, mice were randomly divided into seven groups: a control group treated with 9% sucrose and groups treated with empty PEG-coated cationic liposomes, PEG-coated siNS-lipoplex, PEG-coated siAgo2-lipoplex, S-1, S-1+PEG-coated siNS-lipoplex or S-1+PEG-coated siAgo2-lipoplex. Empty PEG-coated cationic liposomes or PEG-coated siRNA-lipoplexes containing siNS or siAgo2 (48 mg total lipid and 1.6 mg siRNA/kg/injection) were intravenously injected every 2 days (on days 6, 8, 10, 12, 14, 16, 18, and 20). S-1 (tegafur 6.9 mg/kg) was orally administered every day (from day 6 to 20). The tumor volume was measured every other day using a caliper, and tumor volume (cube millimeter) was calculated using the following formula [27]: Tumor volume (cube millimeter)= $1/2 \times \text{length} \times \text{width}^2$. The tumor growth inhibition (TGI (percent)) was calculated using the following equation: TGI (%)=[{1−(tumor growth of treated group on day 21)/(tumor growth of control on day 21)}×100]. Body weight was measured simultaneously.

At 24 h after the last treatment (on day 21), animals were sacrificed and removed tumor tissues. The in vivo gene knockdown effect of treatments was determined by Western blotting. Briefly, tumor tissues were washed with chilled PBS (37 mM NaCl, 2.7 mM KCl, 8.1 mM Na_2HPO_4, and 1.47 mM KH_2PO_4; pH 7.4), homogenized in ice-cold lysis buffer containing 50 mM Tris–HCl (pH 7.4), 1% NP-40, 0.25% sodium deoxycholate, 150 mM NaCl, and protease inhibitor cocktail (Sigma–Aldrich, St Louis, MO, USA). The lysate was collected into a 1.5-ml Eppendorf tube and then centrifuged at 4°C for 15 min at 15,000×g. The protein concentrations in lysates were determined with the Bio-Rad DC Protein Assay kit (Bio-Rad Laboratories, Hercules, CA, USA) with BSA (Sigma–Aldrich) as a standard. Equivalent amounts of protein (27 μg) from each tissue lysate were separated on a 10% SDS-PAGE gel and transferred electrophoretically onto Hybond-ECL (GE Healthcare, Cleveland, CL, USA). The membranes were blocked with Tris-buffered saline containing 0.05% Tween 20 and 5% BSA for 1 h at room temperature and then incubated overnight at 4°C with primary antibodies: mouse anti-mouse Ago2 monoclonal antibody (Wako Pure Chemical, Osaka, Japan) and mouse anti-mouse β-actin monoclonal antibody (Abcam, Cambridge, UK), respectively. β-actin was used as a loading control. After three washes with Tris-buffered saline containing 0.05% Tween 20, membranes were incubated with horseradish peroxidase (HRP)-conjugated goat anti-mouse secondary antibody (MP Biomedicals, Solon, OH, USA) for 1 h at room temperature. After an additional three washes with Tris-buffered saline containing 0.05% Tween 20, membranes were processed for enhanced chemiluminescence using the ECL Plus Chemiluminescence Reagent (GE Healthcare UK Ltd., Little Chalfont, UK), and the obtained images were analyzed using LAS-4000 EPUV-mini and Multi Gauge v.3.2 (Fuji Film, Tokyo, Japan).

Statistical analysis

All values are expressed as the mean±S.D. Statistical analysis was performed with a two-tailed unpaired t test and one-way ANOVA using GraphPad InStat software (GraphPad Software, San Diego, CA, USA). The level of significance was set at $p<0.05$.

Results

Effect of metronomic S-1 dosing on the tumor accumulation and organ biodistribution of PEG-coated siRNA-lipoplexes in a tumor-bearing mice model

The effect of daily S-1 dosing on the accumulation and biodistribution of PEG-coated siRNA-lipoplexes in the LLCC murine solid tumor model was investigated both qualitatively and quantitatively. As shown in Fig. 1, an in vivo imaging study revealed that metronomic S-1 dosing for 7 days substantially enhanced tumor accumulation of fluorescently (DiD)-labeled PEG-coated siRNA-lipoplexes in solid tumor, as compared to the non-treated (control) group. A quantitative study with radioactively labeled lipoplexes showed that pretreatment with metronomic S-1 dosing significantly enhanced tumor accumulation of PEG-coated siRNA-lipoplexes in a treatment duration dependent manner (Fig. 2). Histological examination of the intratumor distribution of PEG-coated siRNA-lipoplexes following 4- and 7-days treatment with metronomic S-1 dosing (Supplementary Fig. 1) supported the intratumor accumulation data. Metronomic S-1 treatment for 7 days significantly allowed broader distribution of PEG-coated siRNA-lipoplexes throughout the tumor tissue compared to either non-treated (control) or 4-days-treated mice. The organ distribution of PEG-coated siRNA-lipoplexes in tumor-bearing mice was also determined following 7-days pretreatment with S-1 dosing (Table 1). At 24 h post-injection, most of the lipoplexes had accumulated in liver and spleen despite the S-1 pretreatment. Very little uptake was observed in other organs such as lung and kidney.

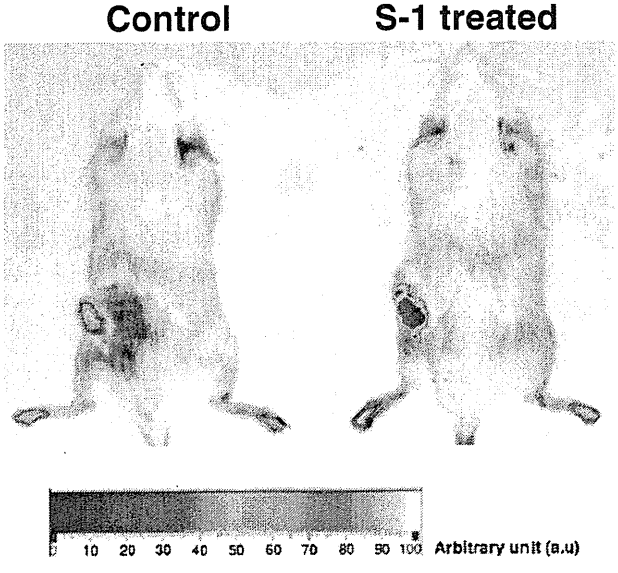

Fig. 1 In vivo imaging of DiD-labeled PEG-coated siRNA-lipoplexes in LLCC tumor-bearing mice. From day 6 after LLCC inoculation, mice were orally treated with or without metronomic S-1 dosing for 7 days and then received DiD-labeled PEG-coated siRNA-lipoplexes intravenously. At 24 h post-injection, in vivo optical images were taken at 1/15-s exposure time. Results shown are representative of three independent experiments

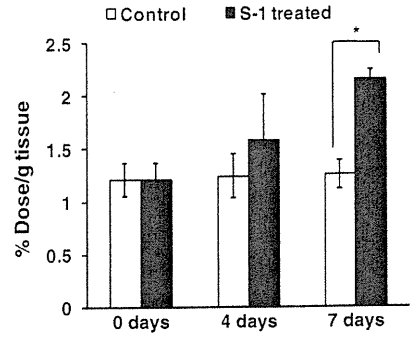

Fig. 2 Tumor accumulation of ^{3}H-CHE-labeled PEG-coated siRNA-lipoplex in LLCC tumor-bearing mice. From day 6 after LLCC inoculation, mice received oral treatment with metronomic S-1 dosing for 4 or 7 days and then injected intravenously with ^{3}H-CHE-labeled PEG-coated siRNA-lipoplexes. At 24 h post-injection, tumor tissue was collected and the radioactivity in the tissue was determined. Data are presented as mean±S.D. (n=5). *p<0.05. Control mice did not receive the S-1 treatment

Effect of metronomic S-1 dosing on intratumoral distribution of PEG-coated siRNA-lipoplexes

To gain more insight into the effect of metronomic S-1 dosing on the intratumoral distribution of PEG-coated siRNA-lipoplexes, histological examination of tumor sections was performed using fluorescence microscopy and whole images of tumor sections as stitched images were qualitatively analyzed. Fluorescence associated with PEG-coated siRNA-lipoplexes was observed in the sections of

Table 1 Biodistribution of ^{3}H-CHE-labeled PEG-coated siRNA-lipoplexes in LLCC tumor-bearing mice

Organ	Control (% dose/g tissue)	S-1 treated (% dose/g tissue)
Blood	1.00±0.44	1.38±0.59
Kidney	1.14±0.13	1.01±0.090
Liver	46.8±10.0	49.4±4.44
Lung	2.38±1.27	1.84±0.94
Spleen	30.5±1.75	30.35±1.68
Tumor	1.25±0.14	2.15±0.34*

LLCC-bearing mice were pretreated with or without oral metronomic S-1 dosing for 7 days and subsequently received ^{3}H-CHE-labeled PEG-coated siRNA-lipoplexes intravenously. At 24 h post-injection, blood, tumor tissue, and major organs (liver, spleen, kidney, and lung) were collected and assayed for radioactivity. Data are presented as mean±S.D (n=5). In the case of spleen, the value was per 250 mg instead of per gram

*p<0.05 compared with control mice

both control (Fig. 3a) and S-1-treated tumor (Fig. 3b). The number and size of fluorescent spots in the section of S-1-treated tumor were substantially larger than those in the section of the control tumor, indicating that S-1 treatment enhanced lipoplex distribution in tumor tissue. Analysis of the strong peaks of fluorescence intensity along the dotted yellow lines in Fig. 3a and b showed that peaks of fluorescence intensity were more frequent in the middle of S-1-treated tumor tissue compared to those in control tumor (Fig. 3c). This indicates that metronomic S-1 dosing results in deeper and broader distribution of PEG-coated siRNA-lipoplexes within the tumor tissue. Interestingly, S-1 dosing resulted in a markedly enhanced accumulation of PEG-coated siRNA-lipoplexes and a far broader distribution around the $CD31^+$ microvessels (Fig. 4).

Antitumor effect of combination therapy of S-1 plus PEG-coated siRNA-lipoplexes

Based on the improved intratumoral delivery of PEG-coated siRNA-lipoplexes by pretreatment with metronomic S-1 dosing, we set out to study the antitumor effect of a combination therapy of S-1 plus PEG-coated siRNA-lipoplexes (Fig. 5). We recently reported that in human fibrosarcoma and several murine cell lines knockdown of the Argonaute2 (Ago2) gene by siRNA for Ago2 (siAgo2) resulted in a potent anti-proliferative effect via the induction of apoptosis [28] and cell cycle arrest in G0/G1 phase. In the present study, siAgo2 was selected as a positive control siRNA while siRNA specific for GFP (non-silencing control siRNA, siNS) was selected as a negative control siRNA. As shown in Fig. 5a, monotherapy with either metronomic S-1 dosing or siAgo2-lipoplexes showed very little antitumor effect. By combination of metronomic S-1 dosing plus siAgo2-lipoplexes, a superior antitumor effect was achieved, as compared to all other treated groups. The index of tumor growth inhibition is presented in Fig. 5b. The data indicate that the combination of the metronomic S-1 dosing plus siAgo2-lipoplexes produced a synergistic antitumor effect (TGI, 71.6%), compared to monotherapy with either S-1 or PEG-coated siAgo2-lipoplexes alone (TGI, 18.2% and 20.2%, respectively) or the sum of the individual tumor growth inhibitory effects of both S-1 and PEG-coated siAgo2-lipoplex (TGI, 38.4%). Throughout the therapeutic experiments, no significant body weight loss was observed in any of the treated groups (Fig. 5c). The Ago2 protein level in the treated tumors was determined by Western blot analysis (Fig. 5d). S-1 treatment did not suppress Ago2 protein

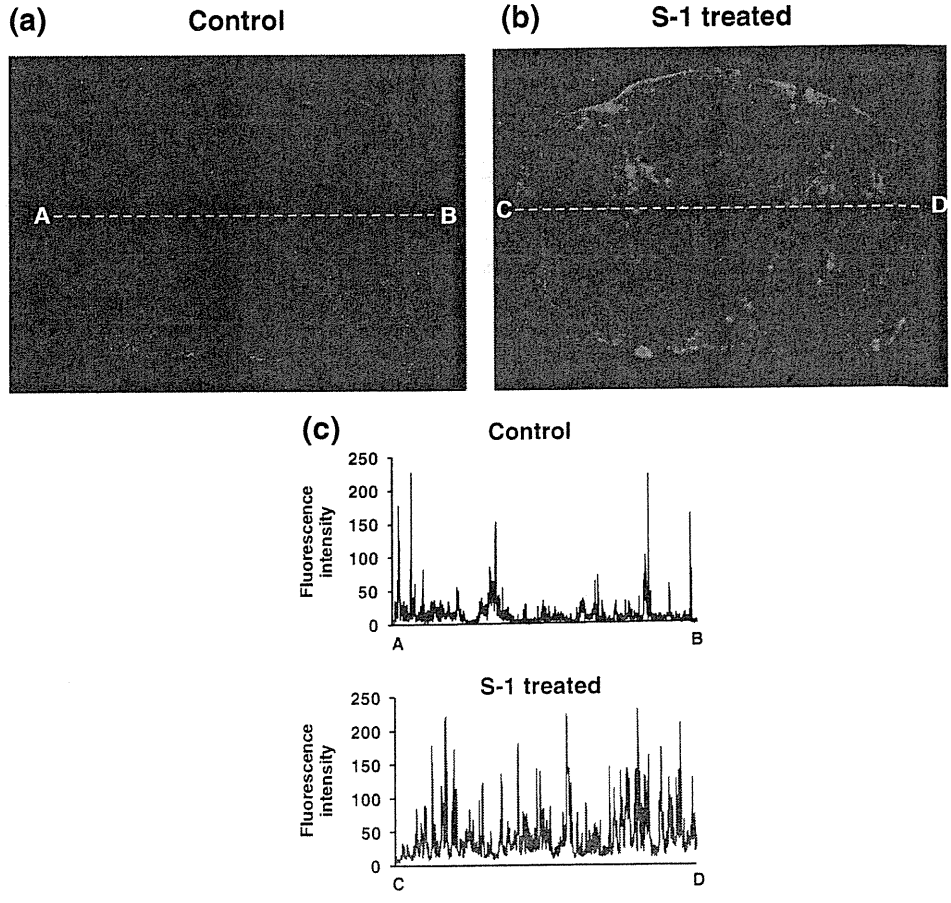

Fig. 3 Intratumoral distribution of DiI-labeled PEG-coated siRNA-lipoplexes in LLCC tumor-bearing mice. LLCC-bearing mice were orally treated with or without metronomic S-1 dosing for 7 days and then received DiI-labeled PEG-coated siRNA-lipoplexes intravenously. At 24 h post-injection, mice were sacrificed and the tumors were excised, snap frozen, and cut into sections. The sections were examined by fluorescence microscopy. **a** Control tumor. **b** S-1-treated tumor. Magnification, ×200. **c** The peaks of fluorescence intensity along the yellow dotted lines in (**a**) and (**b**). The results shown are representative of three independent experiments

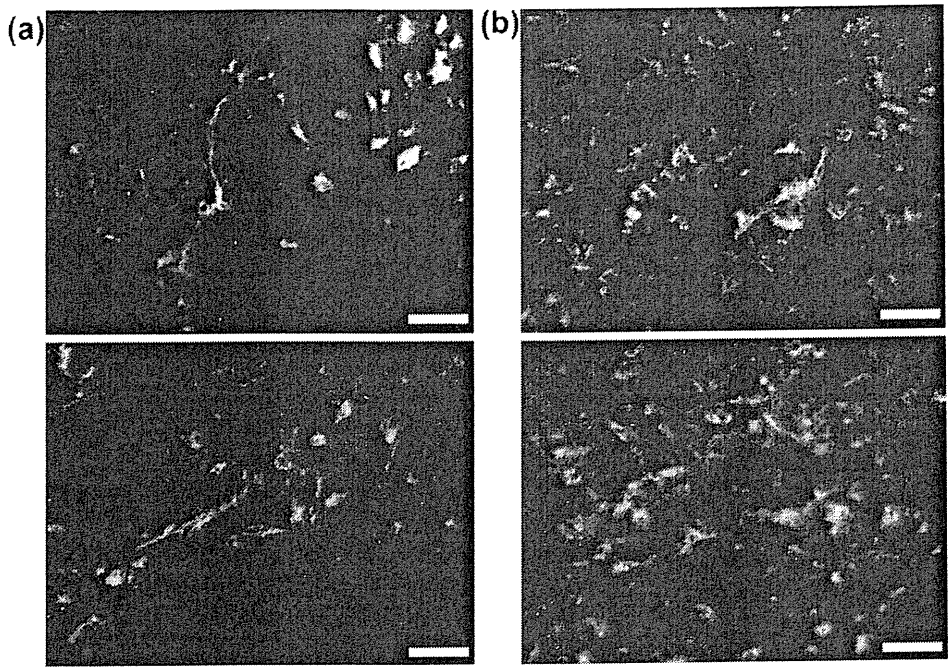

Fig. 4 Intratumoral distribution of DiI-labeled PEG-coated siRNA-lipoplexes along microvessels in LLCC tumor. LLCC-bearing mice were orally treated with or without metronomic S-1 dosing for 7 days and then received DiI-labeled PEG-coated siRNA-lipoplexes intravenously. At 24 h post-injection, the mice were intravenously injected with FITC-conjugated anti-CD31 antibody as microvessel marker. Then, the mice were sacrificed and the tumors were excised, snap frozen, and cut into sections. The sections were examined by fluorescence microscopy. The results shown are representative of three independent experiments. **a** Control tumor. **b** S-1-treated tumor. Red spots represent DiI-labeled PEG-coated siRNA-lipoplexes, Green spots represent $CD31^+$ tumor microvessels and yellow spots represent the co-localization of DiI-labeled PEG-coated siRNA-lipoplexes with the $CD31^+$ microvessels. Scale bar, 50 μm. Magnification, ×100

expression, while treatment with PEG-coated siAgo2-lipoplex induced significant down-regulation of Ago2 protein. The combined treatment with siAgo-2- lipoplex and 5-FU induced further remarkable down-regulation of Ago2 protein expression. In addition, in none of the treatment groups, any change in the level of β-actin expression was observed.

Discussion

RNAi has been widely investigated and has become an emerging potential therapeutic strategy [29–31]. Despite a few promising clinical trials, effective in vivo siRNA delivery remains, however, a major challenge in translating RNAi into the clinical situation as a conventional treatment option. A number of delivery systems and strategies have been developed to circumvent multiple extracellular and intracellular barriers to siRNA delivery in vivo [32–34]. Recently, we proposed a double-modulation strategy to enhance the systemic delivery of PEG-coated siRNA-lipoplexes in tumor and improve their therapeutic efficacy [20]. In the current study, to extend our research, we investigated the effect of metronomic S-1 dosing on the intratumoral accumulation of siAgo2-lipoplexes using LLCC murine solid tumor model.

In vivo imaging (Fig. 1) and histological examination of tumor sections (Fig. 3a and b) revealed that, after metronomic S-1 dosing, intratumoral distribution of PEG-coated siRNA-lipoplexes is substantially enhanced. To gain further insight into the effect of S-1 dosing on the intratumoral distribution of PEG-coated siRNA-lipoplexes, fluorescence images of whole tumor sections were analyzed (Fig. 3c). Regardless of S-1 treatment, strong peaks of fluorescence intensity, which are associated with DiI-labeled PEG-coated siRNA-lipoplexes, were observed along the edges of the tumor sections. Tumors pretreated with metronomic S-1 dosing showed strong peaks of fluorescence intensity (100–200-fold higher than background) at central tumor regions. Control tumor (without S-1 treatment) did not show such strong fluorescence peaks at central regions. In addition, in the S-1-treated tumors, a large number of leaky vessels, which allow extravasation of PEG-coated siRNA-lipoplexes, existed (Fig. 4). These results confirm that by multiple pre-dosing with S-1 substantially enhanced intratumoral accumulation and broader distribution of siRNA-lipoplexes can be achieved, even though they display a substantially larger particle size than PEG-coated neutral liposomes (stealth liposomes). In addition, quantitative evaluation of the effect of pretreatment with metronomic S-1 dosing on the intratumoral accumulation of PEG-coated

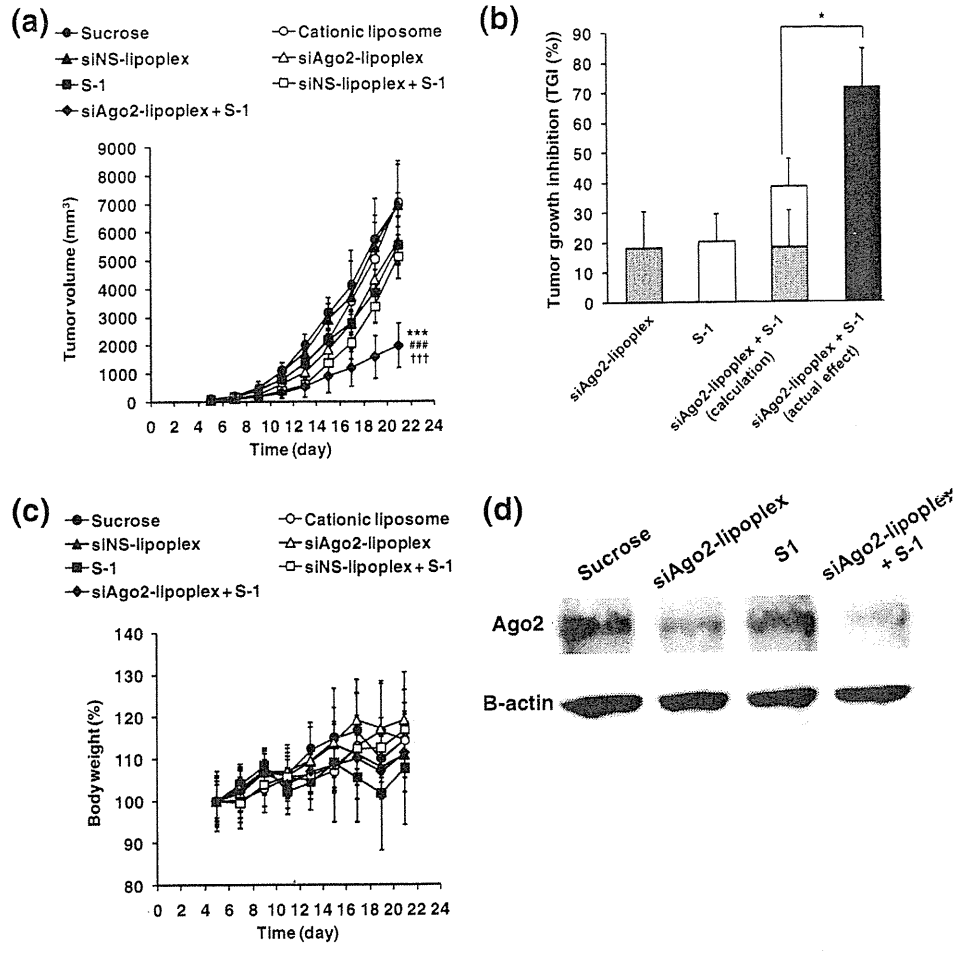

Fig. 5 Antitumor effect of combination therapy of S-1 plus PEG-coated siRNA (siAgo2)-lipoplexes in LLCC tumor-bearing mice. Tumor-bearing mice were pretreated with or without oral metronomic S-1 dosing for 14 days. In parallel with metronomic S-1 dosing, PEG-coated siRNA (siAgo2 or siNS)-lipoplexes was intravenously injected into mice on days 6, 8, 10, 12, 14, 16, 18, and 20 after tumor inoculation. **a** Antitumor effect of each treatment. **b** Tumor growth inhibition (TGI (%)) calculated in day 21. **c** Body weight changes after the different treatments. **d** Ago2 protein expression was determined by Western blot analysis. β-actin protein was used for equal loading assessment. Data in (**a**) represent mean±S.D. (n=6). ***p<0.005 compared with PEG-coated siNS-lipoplex, ###p<0.005 compared with PEG-coated siAgo2-lipoplex, †††p<0.005 compared with S-1

siRNA-lipoplexes also demonstrated a 1.72-fold increase in tumor accumulation of PEG-coated siRNA-lipoplexes upon pretreatment with S-1 dosing, as compared to the non-treated group (Table 1).

Based on the above-mentioned findings, the enhanced intratumoral accumulation and distribution of PEG-coated siRNA-lipoplexes upon pretreatment with metronomic S-1 dosing is assumed to be mediated via alteration of tumor microenvironment. S-1, as a cytotoxic agent, can exert a potent cytotoxic effect on tumor cells and stromal cells and thus could bring about a decrease in the numbers of both cell types [15, 35] and consequently could lead to a decrease in the tumor interstitial pressure and an enlargement of the tumor vasculature and interstitial space. In addition, metronomic chemotherapy has been proven to exert a potent anti-angiogenic effect by targeting genetically stable endothelial cells within the tumor vascular bed resulting in a temporary increase in the gaps between tumor endothelial cells [9, 10]. Accordingly, the increase in the gaps between tumor endothelial cells in conjunction with the decrease in interstitial tumor pressure and enlargement of tumor vasculature and interstitial space, induced by metronomic S-1 dosing, will favor enhanced intratumoral accumulation/distribution of PEG-coated siRNA-lipoplexes. Interestingly, such enhancement effect was not observed after 4 days of metronomic S-1 treatment (Fig. 2 and Supplementary Fig. 1). This suggests that it requires prolonged S-1 treatment to bring about a sufficient change in the intratumoral microenvironment to allow the PEG-coated siRNA-lipoplexes to penetrate deeply and efficiently into the tumor tissue (Figs. 1, 3, and 4). Nevertheless, further investigations to elucidate the exact underlying mechanism on the enhanced intratumoral accumulation and distribution of PEG-coated siRNA-lipoplexes upon pretreatment with metronomic S-1 dosing should be required.

Combination therapy of metronomic S-1 dosing and PEG-coated siRNA-lipoplexes could provide superior tumor growth suppression, compared to monotherapy with either S-1 dosing or PEG-coated siRNA-lipoplex alone (Fig. 5a). In this therapeutic experiment, we selected siRNA against the Ago2 (siAgo2) gene as a positive control. It is well known that Ago2 is the key protein in mammalian RNAi and mediates the microRNA (miRNA)-dependent cleavage of targeted mRNAs. We recently reported that

Ago2 gene knockdown suppresses cellular proliferation in human fibrosarcoma (HT-1080) and HUVEC [28]. We here confirm that Ago2 knockdown induces inhibition of proliferation of LLCC (Supplementary Figure 2). This might be due to transient inhibition of miRNA-targeted mRNAs resulting in the induction of apoptosis and cell cycle arrest in G0/G1 phase. In the present study, we found the potent antitumor activity of the combination of S-1 dosing and PEG-coated siAgo2-lipoplexes to be synergistic (Fig. 5b). This synergistic antitumor activity might be due to the following tentative mechanism: pretreatment with metronomic S-1 dosing results in a preferential intratumoral accumulation, along with cytotoxic action on tumor cells and endothelial cells, and permits efficient delivery of siAgo2-lipoplexes into the tumor tissue and thereby potentiates the apoptotic effects of the accumulated siAgo2-lipoplexes as a result of significant down-regulation of Ago2 protein in the tumor tissue (Fig. 5d). Interestingly, no body weight changes were observed with the combination therapy of S-1 and PEG-coated siAgo2-lipoplexes (Fig. 5c). This might be attributed to the targeted delivery of siAgo2-lipoplexes to tumor tissues which allows enhanced accumulation of siAgo2-lipolexes in tumor tissues (Table 1).

One of the major hurdles for intratumoral drug delivery is the heterogeneity of tumor tissue. The abnormalities in vessel and microenvironment of solid tumors will often result in insufficient drug delivery and therapeutic efficiency [36]. To improve drug delivery to the disordered tumor microenvironment and increase therapeutic efficacy, various approaches have been applied. For example, it has been reported that the combination of physical power (radiation [37], ultrasound [38], mild hyperthermia [39], and chemical drug (TβR-1 [40], TNF-α [41])) improved the intratumoral distribution of nanoparticles. In the current study, we utilized a novel approach for improving the delivery of siRNA-lipoplexes to tumor tissue. This approach using a clinically approved anticancer drug, S-1, is considered a breakthrough in gene delivery strategies and is hopefully translated into clinical settings.

Conclusion

In this study, we showed that the metronomic S-1 dosing improved the intratumoral accumulation and distribution of PEG-coated siAgo2-lipoplexes and, as a result, significantly improved the overall therapeutic efficacy of the combination of these two treatments. The improved delivery of PEG-coated siRNA-lipoplexes was presumably mediated by alterations in tumor microenvironment brought about by the S-1 treatment. The current study serves as a positive proof-of-concept demonstration for the enhanced systemic delivery of PEG-coated siRNA-lipoplexes upon combination with metronomic S-1 chemotherapy we assumed recently [20]. Moreover, combination of a chemotherapeutic agent and siRNA-based therapy, two therapeutic strategies with different mechanisms of action, constitutes a promising approach for the development of novel strategies in cancer therapy.

Acknowledgments We thank Dr. G. L. Scherphof for his helpful advice in preparing this manuscript. This study was supported in part by Daiwa Securities Health Foundation, Mochida Memorial Foundation for Medical and Pharmaceutical Research, a Grant-in-Aid for Young Scientists (A) (21689002), the Ministry of Education, Culture, Sports, Science and Technology, Japan and by the Health and Labour Sciences Research Grants for Research on Advanced Medical Technology from the Ministry of Health, Labour and Welfare of Japan.

References

1. Meister G, Landthaler M, Patkaniowska A, Dorsett Y, Teng G, Tuschl T. Human Argonaute2 mediates RNA cleavage targeted by miRNAs and siRNAs. Mol Cell. 2004;15:185–97.
2. Akhtar S, Benter IF. Nonviral delivery of synthetic siRNAs in vivo. J Clin Invest. 2007;117:3623–32.
3. Phalon C, Rao DD, Nemunaitis J. Potential use of RNA interference in cancer therapy. Expert Rev Mol Med. 2010;12:e26.
4. Haupenthal J, Baehr C, Kiermayer S, Zeuzem S, Piiper A. Inhibition of RNAse A family enzymes prevents degradation and loss of silencing activity of siRNAs in serum. Biochem Pharmacol. 2006;71:702–10.
5. Kim WJ, Chang CW, Lee M, Kim SW. Efficient siRNA delivery using water soluble lipopolymer for anti-angiogenic gene therapy. J Control Release. 2007;118:357–63.
6. Yano J, Hirabayashi K, Nakagawa S, Yamaguchi T, Nogawa M, Kashimori I, et al. Antitumor activity of small interfering RNA/cationic liposome complex in mouse models of cancer. Clin Cancer Res. 2004;10:7721–6.
7. Santel A, Aleku M, Keil O, Endruschat J, Esche V, Fisch G, et al. A novel siRNA-lipoplex technology for RNA interference in the mouse vascular endothelium. Gene Ther. 2006;13:1222–34.
8. Shim MS, Kwon YJ. Efficient and targeted delivery of siRNA in vivo. FEBS J. 2010;277:4814–27.
9. Kerbel RS, Kamen BA. The anti-angiogenic basis of metronomic chemotherapy. Nat Rev Cancer. 2004;4:423–36.
10. Laquente B, Vinals F, Germa JR. Metronomic chemotherapy: an antiangiogenic scheduling. Clin Transl Oncol. 2007;9:93–8.
11. Sanchez-Munoz A, Mendiola C, Perez-Ruiz E, Rodriguez-Sanchez CA, Jurado JM, Alonso-Carrion L, et al. Bevacizumab plus low-dose metronomic oral cyclophosphamide in heavily pretreated patients with recurrent ovarian cancer. Oncology. 2010;79:98–104.
12. Correale P, Remondo C, Carbone SF, Ricci V, Migali C, Martellucci I, et al. Dose/dense metronomic chemotherapy with fractioned cisplatin and oral daily etoposide enhances the anti-angiogenic effects of bevacizumab and has strong antitumor activity in advanced non-small-cell-lung cancer patients. Cancer Biol Ther. 2010;9:685–93.
13. Sperone P, Ferrero A, Daffara F, Priola A, Zaggia B, Volante M, et al. Gemcitabine plus metronomic 5-fluorouracil or capecitabine as a second-/third-line chemotherapy in advanced adrenocortical carcinoma: a multicenter phase II study. Endocr Relat Canc. 2010;17:445–53.
14. Tang TC, Man S, Lee CR, Xu P, Kerbel RS. Impact of metronomic UFT/cyclophosphamide chemotherapy and antiangiogenic drug

assessed in a new preclinical model of locally advanced orthotopic hepatocellular carcinoma. Neoplasia. 2010;12:264–74.
15. Ooyama A, Oka T, Zhao HY, Yamamoto M, Akiyama S, Fukushima M. Anti-angiogenic effect of 5-fluorouracil-based drugs against human colon cancer xenografts. Cancer Lett. 2008;267:26–36.
16. Sakuramoto S, Sasako M, Yamaguchi T, Kinoshita T, Fujii M, Nashimoto A, et al. Adjuvant chemotherapy for gastric cancer with S-1, an oral fluoropyrimidine. N Engl J Med. 2007;357:1810–20.
17. Shiraga E, Barichello JM, Ishida T, Kiwada H. A metronomic schedule of cyclophosphamide combined with PEGylated liposomal doxorubicin has a highly antitumor effect in an experimental pulmonary metastatic mouse model. Int J Pharm. 2008;353:65–73.
18. Ishida T, Shiraga E, Kiwada H. Synergistic antitumor activity of metronomic dosing of cyclophosphamide in combination with doxorubicin-containing PEGylated liposomes in a murine solid tumor model. J Control Release. 2009;134:194–200.
19. Doi Y, Okada T, Matsumoto H, Ichihara M, Ishida T, Kiwada H. Combination therapy of metronomic S-1 dosing with oxaliplatin-containing polyethylene glycol-coated liposome improves antitumor activity in a murine colorectal tumor model. Cancer Sci. 2010;101:2470–5.
20. Nakamura K, Abu Lila AS, Matsunaga M, Doi Y, Ishida T, Kiwada H. A double-modulation strategy in cancer treatment with a chemotherapeutic agent and siRNA. Mol Ther. 2011;19:2040–7.
21. Suzuki K, Kokuryo T, Senga T, Yokoyama Y, Nagino M, Hamaguchi M. Novel combination treatment for colorectal cancer using Nek2 siRNA and cisplatin. Cancer Sci. 2010;101:1163–9.
22. Tagami T, Hirose K, Barichello JM, Ishida T, Kiwada H. Global gene expression profiling in cultured cells is strongly influenced by treatment with siRNA-cationic liposome complexes. Pharm Res. 2008;25:2497–504.
23. Tagami T, Nakamura K, Shimizu T, Ishida T, Kiwada H. Effect of siRNA in PEG-coated siRNA-lipoplex on anti-PEG IgM production. J Control Release. 2009;137:234–40.
24. Bartlett GR. Colorimetric assay methods for free and phosphorylated glyceric acids. J Biol Chem. 1959;234:469–71.
25. Ishida T, Iden DL, Allen TM. A combinatorial approach to producing sterically stabilized (Stealth) immunoliposomal drugs. FEBS Lett. 1999;460:129–33.
26. Harashima H, Yamane C, Kume Y, Kiwada H. Kinetic analysis of AUC-dependent saturable clearance of liposomes: mathematical description of AUC dependency. J Pharmacokinet Biopharm. 1993;21:299–308.
27. Abu Lila AS, Kizuki S, Doi Y, Suzuki T, Ishida T, Kiwada H. Oxaliplatin encapsulated in PEG-coated cationic liposomes induces significant tumor growth suppression via a dual-targeting approach in a murine solid tumor model. J Control Release. 2009;137:8–14.
28. Tagami T, Suzuki T, Matsunaga M, Nakamura K, Moriyoshi N, Ishida T, et al. Anti-angiogenic therapy via cationic liposome-mediated systemic siRNA delivery. Int J Pharm. 2011;422(1–2):280–9.
29. Tan FL, Yin JQ. RNAi, a new therapeutic strategy against viral infection. Cell Res. 2004;14:460–6.
30. Orlacchio A, Bernardi G, Martino S. RNA interference as a tool for Alzheimer's disease therapy. Mini Rev Med Chem. 2007;7:1166–76.
31. Khaliq S, Khaliq SA, Zahur M, Ijaz B, Jahan S, Ansar M, et al. RNAi as a new therapeutic strategy against HCV. Biotechnol Adv. 2010;28:27–34.
32. Aigner A. Delivery systems for the direct application of siRNAs to induce RNA interference (RNAi) in vivo. J Biomed Biotechnol. 2006;2006:71659.
33. Kim SH, Jeong JH, Kim TI, Kim SW, Bull DA. VEGF siRNA delivery system using arginine-grafted bioreducible poly(disulfide amine). Mol Pharm. 2009;6:718–26.
34. Hauser PV, Pippin JW, Kaiser C, Krofft RD, Brinkkoetter PT, Hudkins KL, et al. Novel siRNA delivery system to target podocytes in vivo. PLoS One. 2010;5:e9463.
35. Finak G, Laferriere J, Hallett M, Park M. The tumor microenvironment: a new tool to predict breast cancer outcome. Med Sci (Paris). 2009;25:439–41.
36. Jain RK. Normalization of tumor vasculature: an emerging concept in antiangiogenic therapy. Science. 2005;307:58–62.
37. Davies Cde L, Lundstrom LM, Frengen J, Eikenes L, Bruland SO, Kaalhus O, et al. Radiation improves the distribution and uptake of liposomal doxorubicin (caelyx) in human osteosarcoma xenografts. Cancer Res. 2004;64:547–53.
38. Deckers R, Moonen CT. Ultrasound triggered, image guided, local drug delivery. J Control Release. 2010;148:25–33.
39. Koning GA, Eggermont AM, Lindner LH, ten Hagen TL. Hyperthermia and thermosensitive liposomes for improved delivery of chemotherapeutic drugs to solid tumors. Pharm Res. 2010;27:1750–4.
40. Kano MR, Bae Y, Iwata C, Morishita Y, Yashiro M, Oka M, et al. Improvement of cancer-targeting therapy, using nanocarriers for intractable solid tumors by inhibition of TGF-beta signaling. Proc Natl Acad Sci U S A. 2007;104:3460–5.
41. Ten Hagen TL, Van Der Veen AH, Nooijen PT, Van Tiel ST, Seynhaeve AL, Eggermont AM. Low-dose tumor necrosis factor-alpha augments antitumor activity of stealth liposomal doxorubicin (DOXIL) in soft tissue sarcoma-bearing rats. Int J Cancer. 2000;87:829–37.

International Journal of Pharmaceutics 430 (2012) 359–365

Contents lists available at SciVerse ScienceDirect

International Journal of Pharmaceutics

journal homepage: www.elsevier.com/locate/ijpharm

Pharmaceutical Nanotechnology

Agitation during lipoplex formation harmonizes the interaction of siRNA to cationic liposomes

José Mario Barichello[a,d,1], Shinji Kizuki[a], Tatsuaki Tagami[a], Luiz Alberto Lira Soares[b], Tatsuhiro Ishida[a,*], Hiroshi Kikuchi[c], Hiroshi Kiwada[a]

[a] Department of Pharmacokinetics and Biopharmaceutics, Institute of Health Biosciences, The University of Tokushima, 1-78-1 Sho-machi, Tokushima, Japan
[b] Departamento de Farmácia, Universidade Federal do Rio Grande do Norte, Natal, Brazil
[c] Eisai Co. Ltd., Tokyo, Japan
[d] Japan Association for the Advancement of Medical Equipment, Tokyo, Japan

ARTICLE INFO

Article history:
Received 16 January 2012
Received in revised form 7 March 2012
Accepted 5 April 2012
Available online 12 April 2012

Keywords:
siRNA
Lipoplex preparation procedure
FRET
Circular dichroism
Vortex-mixing
Gene knockdown effect

ABSTRACT

We recently demonstrated that agitation during lipoplex formation (vorLTsiR) improves the gene knockdown effect of siRNA because the resultant decrease in lipoplex size leads to an enhanced uptake by cells. In furthering this line of research, the present study was focused on the interaction of siRNA to cationic liposomes during lipoplex preparation. A fluorescence resonance energy transfer (FRET) study indicated that the application of agitation in the presence of siRNA effectively reorganized positively charged lipids (DC-6-14 and DOPE) in an order that effectively promoted further electrostatic interaction between the negatively charged phosphate backbone of siRNA and the positively charged lipids in the cationic liposome membrane. A circular dichroism (CD) study indicated that the agitation did not bring about a change in the A-form helix of siRNA, therefore the interactions between the lateral anionic groups of siRNA – responsible for the characteristic bands of the A-form helix – and cationic liposomes were effectively promoted. Factorial design coupled with response surface methodology was used to statistically analyze the influence of vortex speed and time and siRNA dose on the *in vitro* gene knockdown effects of siRNA-lipoplex that were spontaneously formulated (spoLTsiR) along with that formulated under agitation (vorLTsiR). The analysis indicated that vortex speed plays the most important role in enhancing the gene knockdown effect of siRNA among the three variables, although all three are important. It was concluded that the high energy transmitted by applying agitation during lipoplex formation harmonized the interaction of siRNA to positively charged lipids (DC-6-14 and DOPE) in cationic liposomes, resulting in a superior gene knockdown efficacy of vorLTsiR compared to spoLTsiR. Our study suggests that the preparation procedure is one of the critical factors in producing the enhanced gene knockdown effect of siRNA.

1. Introduction

RNA interference (RNAi), the naturally occurring biological process of gene silencing in mammalian cells, has emerged as a promising therapeutic strategy for treating malignant, infectious and autoimmune diseases (Li et al., 2006). Cationic liposomes are non-viral vectors that can complex with negatively charged siRNA duplexes, allowing these molecules to overcome the electrostatic repulsion of the cell membrane and to be taken up by the targeted cells (Lasic and Templeton, 1996; Lima et al., 2001).

It is well known that the preparation procedure strongly determines the final physicochemical features of the pDNA–cationic liposome complex (lipoplex) that modulate its biological activity (Lasic and Templeton, 1996; Lima et al., 2001). Lipoplexes are generally formed spontaneously through the electrostatic interaction between the positively charged lipids of liposomes and the negatively charged phosphate backbones of nucleic acids (Lasic and Templeton, 1996). We recently demonstrated that the application of vortex-mixing (agitation) during lipoplex formation considerably improves the gene knockdown effect of siRNA. The efficacy of the lipoplex formulated by agitation (vorLTsiR) was superior to the lipoplex formed spontaneously (spoLTsiR) in the same siRNA dose (Barichello et al., 2011). Vortex mixers are often used in bioscience laboratories to mix reagents in solution or suspension. They quickly create a vigorous vortex, a spiral flow, inside the liquid mixture. However, when the lipoplex preparation procedure is varied from

* Corresponding author. Tel.: +81 88 633 7260; fax: +81 88 633 7260.
E-mail address: ishida@ph.tokushima-u.ac.jp (T. Ishida).
[1] Current address: Laboratory of Nanobiotechnology, School of Pharmacy, Universidade Federal de Ouro Preto (UFOP), 35400-000 Ouro Preto, MG, Brazil.

0378-5173/$ – see front matter © 2012 Elsevier B.V. All rights reserved.
http://dx.doi.org/10.1016/j.ijpharm.2012.04.006

static (spontaneous formation) to dynamic (under vortex-mixing) it is unknown what the associated behavior of siRNA to a cationic liposome will be, nor do we know the implications for the gene knockdown effect of siRNA.

In an expansion of our recent study, in this study, we investigated the effect of the lipoplex preparation procedure on the behavior of siRNA as it associates with a cationic liposome by using fluorescence resonance energy transfer (FRET) and circular dichroism (CD). Then, we determined the effect of the three variables (vortex speed and time and siRNA dose) on the gene knockdown effect of siRNA lipoplex using an *in vitro* luciferase gene knockdown assay system with HeLa cells. To determine which was the most important variable among the three, a statistical analysis was undertaken with a 3^3 full factorial design and response surface methodology, which is a widely used statistical tool for the systematic and effective evaluation of influences from differences among variables (Dillen et al., 2004; Gonzalez-Rodriguez et al., 2007). Herein, we show that the preparation procedure has far-reaching implications for the behavior of siRNA as it associates with a cationic liposome, and, therefore, for the final physicochemical features of a lipoplex and for the gene knockdown effect of siRNA in target cells.

2. Materials and methods

2.1. Materials

The cationic liposome, LipoTrust™-SR (LT), composed of *O,O'*-ditetradecanoyl-*N*-(α-trimethyl ammonioacetyl) diethanolamine chloride (DC-6-14), dioleoylphosphatidylethanolamine (DOPE) and cholesterol in a molar ratio of 1.00/0.75/0.75, was purchased from Hokkaido System Science (Hokkaido, Japan). The 1% Lissamine™ rhodamine B 1,2-dihexadecanoyl-sn-glycero-3-phosphoethanolamine (Rho-DOPE)-containing LipoTrust™-SR (Rho-LT) was a generous gift from Daiichi-Sankyo Pharmaceutical (Tokyo, Japan). All other chemicals were of reagent grade and used as received.

2.2. siRNA preparation

A siRNA for firefly luciferase (siLuc) (sense sequence, 5′-CUUACGCUGAGUACUUCGATT-3′; antisense sequence 5′-UCGAAGUACUCAGCGUAAGTT-3′) and an unrelated siRNA (sense sequence, 5′-AGCUUCAUAAGGCGCAUGCTT-3′; antisense sequence 5′-GCAUGCGCCUUAUGAAGCUTT-3′) (Elbashir et al., 2001) were chemically synthesized and purified with HPLC by Hokkaido System Science (Hokkaido, Japan). The siLuc labeled at the 5′-end of the sense strand with carboxyfluorescein (FAM) (FAM-siLuc) was used as a fluorescent siRNA probe. For siRNA preparation, the complementary antisense and sense strands were mixed in TE buffer (10 μM Tris–HCl, 1 μM EDTA (pH 8.0), DNase and RNase free grade, Nippon Gene, Tokyo, Japan) in a 1:1 molar ratio followed by heating at 90 °C for 1 min. The reaction was then allowed to cool to room temperature. The quality of siRNA was checked by 15% PAGE. The final concentration of the duplexes was 50 μM in a TE buffer.

2.3. Preparation of siRNA lipoplex

Various aliquots of the siRNA solution (50 μM) were diluted to a final volume of 100 μl with fresh Opti-MEM (Invitrogen, CA, USA) or 9% sucrose. A 25 μl aliquot of LT suspension (2.4 μM) was also diluted to a final volume of 100 μl with fresh Opti-MEM or 9% sucrose. The diluted siRNA solutions were then mixed with the diluted LT suspension. The N/P ratios were set at 7.62 (9.6 μM/30.0 nM; cationic lipid$^+$/siRNA$^-$) for FRET and CD experiments, while for the 3^3 full-factorial design, the N/P ratios were set at 0.95, 1.90 and 3.81 (9.6 μM/1.88, 3.75 and 7.50 nM; cationic lipid$^+$/siRNA$^-$; respectively) to evaluate the effect of LTsiRNA lipoplex (LTsiR) preparation. The LTsiR was allowed to form in 2 ways: the lipoplex was formed spontaneously (spoLTsiR) by allowing samples to stand for 10 min, and it also was formed under application of high vortex-mixing (2500 rpm) (vorLTsiR) (Vortex-Genie 2, Scientific Industries, NY, USA) for 10 min (Barichello et al., 2011).

2.4. Fluorescence resonance energy transfer (FRET)

FRET was determined by monitoring the decrease in fluorescence of FAM-siLuc (donor) in the presence of Rho-DOPE in LT (acceptor) using a fluorescence spectrophotometer Jasco FP6600 (JASCO, Tokyo, Japan). Emission spectra were recorded between 500 and 650 nm with excitation at 505 nm at 25 °C immediately after the complexes were formed. Data are reported as the efficiency of FRET (E) (which is calculated as follows: $E = [1 - (F_{DA}/F_D)] \times 100$, where F_{DA} and F_D are the fluorescence intensity of the FAM-siLuc (excitation at 505 nm and emission at 525 nm) in the presence of Rho-LT and LT, respectively (Zelphati and Szoka, 1996). The Rho fluorescence value (I) was computed as $I = [F'_{DA}/(F'_D + F'_A)] \times 100$, where F' is the fluorescence intensity of the Rho-DOPE in LT (excitation at 505 nm and emission at 588 nm) in the presence of Rho-LT and FAM-siLuc (F'_{DA}), LT and FAM-siLuc (F'_D), and Rho-LT and siLuc (F'_A) (Zelphati and Szoka, 1996).

2.5. Circular dichroism (CD)

CD spectra were collected at 25 °C using a spectropolarimeter Jasco J600 (Tokyo, Japan). Spectra were measured from 200 to 300 nm with a resolution of 1 nm using a 2 mm path length cuvette and were expressed as the average of 8 scans at a 20 nm/min scan rate. The spectrum of siRNA (30 nM) and LT (9.6 μM) alone, and the spectra of their complex were taken. The complexes formed in 9% sucrose and the spectrum of 9% sucrose were recorded as a control, which was subtracted. Data analysis was performed using Excel 2003 (Microsoft, Redmond, WA, USA).

2.6. The in vitro luciferase gene knockdown assay

The human cervical cancer (HeLa) cell line was obtained from Dr. Y. Shinohara (Division of Gene Expression, Institute of Genome Research, The University of Tokushima, Japan). HeLa cells were cultured in DMEM (Sigma, MO, USA) supplemented with 10% (v/v) heat-inactivated FBS, 100 IU/ml penicillin and 100 μg/ml streptomycin (ICN Biomedical, OH, USA) at 37 °C in a humidified atmosphere of 5% CO_2/95% air. The cells were maintained in exponential growth.

Two luciferase plasmids (*Photinus* (firefly), luciferase pGL-3 and *Renilla* (sea pansy) luciferase, pRL-TK) were used as reporter and control genes, respectively, by a reported transfection protocol with modifications (Elbashir et al., 2001). Typically, the complex of pDNA-LT was prepared at a ratio of 1 μg of pDNA to 5 μmol of cationic lipid (the molar charge ratio (N/P) was 1.33) in Opti-MEM medium as previously described (Li et al., 2004). The cells were seeded in 24-well plates at a density of 5.0×10^4 cells/well for 24 h prior to transfection. The growth medium was removed and replaced with 146.7 μl of Opti-MEM, 20 μl of FBS and 33.3 μl of pDNA-LT to transfect. After incubation for 1 h, the transfection medium was removed and replaced with 410 μl of Opti-MEM, 50 μl of FBS and 40 μl of LTsiR. The plates were incubated for another 4 h. The lipofection medium was then removed and replaced with 500 μl of fresh DMEM containing 10% FBS, and the plates were

Table 1
The experimental design.

Trial	Variable levels			F-luc/R-luc (% control)
	X_1	X_2	X_3	
1	3.75	0	2	92.0 ± 13.2
2	3.75	0	5	89.1 ± 4.4
3	3.75	0	10	89.1 ± 14.9
4	3.75	800	2	84.2 ± 6.6
5	3.75	800	5	78.3 ± 4.1
6	3.75	800	10	73.4 ± 5.1
7	3.75	2500	2	75.3 ± 12.0
8	3.75	2500	5	60.5 ± 1.9
9	3.75	2500	10	38.2 ± 1.8
10	7.50	0	2	82.9 ± 4.9
11	7.50	0	5	76.2 ± 4.3
12	7.50	0	10	70.9 ± 1.9
13	7.50	800	2	81.0 ± 9.9
14	7.50	800	5	63.9 ± 4.7
15	7.50	800	10	59.9 ± 10.2
16	7.50	2500	2	72.1 ± 12.0
17	7.50	2500	5	48.9 ± 5.1
18	7.50	2500	10	28.9 ± 1.8
19	15.00	0	2	64.3 ± 2.7
20	15.00	0	5	64.5 ± 0.9
21	15.00	0	10	58.9 ± 3.9
22	15.00	800	2	76.3 ± 10.0
23	15.00	800	5	52.1 ± 8.7
24	15.00	800	10	42.7 ± 6.9
25	15.00	2500	2	58.2 ± 3.2
26	15.00	2500	5	48.3 ± 5.7
27	15.00	2500	10	31.9 ± 2.3

X_1 = dose of siRNA (nM); X_2 = vortex speed (rpm); X_3 = vortex time (min).

incubated for another 20 h. Cells were then harvested at 24 h post-lipofection of siRNA using a passive lysis buffer (100 μl/well), according to instructions, with minor modifications, that was provided with the Dual-Luciferase Reporter Assay System (Promega, WI, USA). The luciferase activities of the samples were measured using a BLR-301 luminometer (Aloka, Tokyo, Japan), with a delay time of 2 s and an integrate time of 10 s. The inhibitory effect on luciferase activities by siLuc was expressed as the percentage of the normalized ratios between the luciferase activities of the reporter and control genes (F-Luc/R-Luc) (Elbashir et al., 2001; Xu et al., 2003). All experiments were performed in quadruplicate and were repeated at least twice.

2.7. Statistical analysis with a 3^3 full-factorial design

Elements of the experimental design of *in vitro* luciferase gene knockdown, siRNA dose (nM), vortex speed (rpm), and vortex time (min), are summarized in Table 1. Calculations of the effects and their statistical interpretation, as well as the response surface, were performed using the software STATISTICA 6.1 (StatSoft, OK, USA). To determine the relationship between the 3 controlled variables and the luciferase gene knockdown effect, the experimental data was adjusted to a second-order model shown by the following Eq. (1):

$$Y = b_0 + \Sigma b_i X_i + \Sigma b_{ij} X_i X_j + \Sigma b_{ii} X_i^2 \quad (1)$$

For the 3 variables, the following equation model (Eq. (2)) applies:

$$Y = b_0 + b_1X_1 + b_2X_2 + b_3X_3 + b_{12}X_1X_2 + b_{13}X_1X_3 + b_{23}X_2X_3 + b_{11}(X_1)^2 + b_{22}(X_2)^2 + b_{33}(X_3)^2 \quad (2)$$

where b_0 is the arithmetic mean response of 27 runs and $b_1 \ldots b_{33}$ are the estimated coefficients for the 3 factors (X_1, dose of siRNA; X_2, vortex speed and X_3, vortex time).

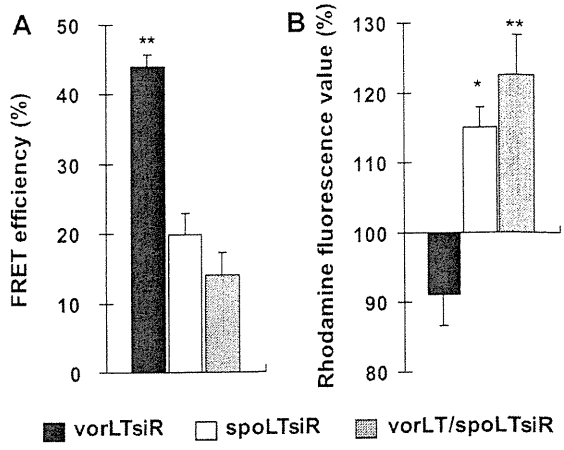

Fig. 1. Effect of the lipoplex preparation procedure on FRET efficiency (E) and rhodoamine fluorescence values (I). *Legend*: vorLT/spoLTsiR, LT alone was vortexed for 10 min followed by spontaneous lipoplex formation after addition of siRNA. Cationic lipid$^+$/siRNA$^-$ ratio was 9.6 μM/30 nM, which corresponds to a charge ratio of 7.62. Data represent the mean ± S.D. of 5 independent experiments. $^{**}P < 0.01$; significant difference in the mean E of vorLTsiR compared with that of spoLTsiR and vorLT/spoLTsiR. $^{**}P < 0.01$ and $^{*}P < 0.05$; significant difference in the mean I of vorLTsiR compared with that of spoLTsiR and vorLT/spoLTsiR, respectively.

The regression analysis was carried out using Eq. (3):

$$\begin{aligned}\text{RNAi effect(F-luc/R-luc)} = {} & 67.08 - 10.16[X_1] - 12.54[X_2] \\ & -10.69[X_3] + 3.91[X_1][X_2] \\ & -1.20[X_1][X_3] - 7.17[X_2][X_3] \\ & +0.42[X_1]^2 - 2.04[X_2]^2 + 0.91[X_3]^2 \quad (3)\end{aligned}$$

where X_1, X_2 and X_3 represent the main effects, dose of siRNA, vortex speed and vortex time, respectively.

Calculations were performed using the least-square method and validation was performed through ANOVA, multiple-correlation coefficient and estimation of the lack of fit using the criteria proposed by Wherle et al. (1995). Response surface methodology was used to understand as fully as possible the effects and levels of the valuables, and to predict the response inside the experimental domain.

2.8. Statistical analysis

Statistical analyses (one-way ANOVA and unpaired t-test) were performed using Graph Pad Stat View software (Abacus Concepts Inc., CA, USA). This evaluation was carried out at the N/P ratio of 7.62 (9.6 μM/30 nM; cationic lipid (L)$^+$/siRNA$^-$) wherein the most distinct difference in the RNAi effect between the lipoplex preparation procedures was observed (Barichello et al., 2011).

3. Results

3.1. FRET study to evaluate the behavior of the association of siRNA to a cationic liposome

FRET was employed to evaluate the behavior of the association of siRNA to a cationic liposome during the preparation process. As shown in Fig. 1A, the FRET between FAM-siRNA and Rho-labeled cationic liposome occurred regardless of the preparation procedure (Fig. 1A). The FRET efficiency of vorLTsiR was 2.2-fold higher than that of spoLTsiR, indicating that application of agitation further promoted the effective interaction of FAM-labeled siRNA with Rho-labeled cationic liposome. Interestingly, the addition of siRNA following application of agitation to cationic liposome for 10 min

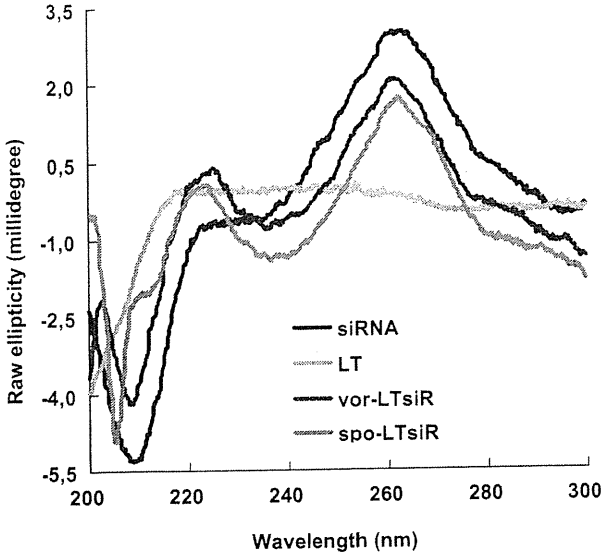

Fig. 2. Effect of preparation procedure on the CD spectra of siRNA in the lipoplex. Cationic lipid$^+$/siRNA$^-$ ratio was 9.6 μM/30 nM, which corresponds to a charge ratio of 7.62. The data are typical of 3 independent experiments.

did not increase the FRET efficiency. This demonstrates the importance of the presence of siRNA in promoting an efficient membrane lipid mixture and consequent efficient interaction between siRNA and the surface of a cationic liposome.

It is generally believed that nucleic acids associate with cationic lipids in a cationic liposome. In the present study, it was assumed that DC-6-14 is the major positively charged lipid that associates with siRNA. However, the Rho fluorescence value was decreased for vorLTsiR, while that of spoLTsiR was increased (Fig. 1B). Because Rho is covalently bound to DOPE, the Rho fluorescence value might reflect free DOPE in the membrane of cationic liposome. Thus, not only DC-6-14 but also DOPE in the membrane participated with siRNA interaction in vorLTsiR (Fig. 1A). The addition of siRNA following application of agitation to cationic liposome for 10 min slightly increased the Rho fluorescence value (Fig. 1B). This indicates the importance of the present of siRNA during agitation to promote the homogeneous distribution of DOPE and DC-6-14 in the membrane.

3.2. CD study for evaluation of the behavior of siRNA association to a cationic liposome

The spectrum of siRNA alone presented a large positive band at 260 nm and a large negative band at 208 nm (Fig. 2), which readily characterized the A-form helix of a double-stranded RNA. The CD spectrum of a cationic liposome (LT) alone showed no band at these wavelengths. In the spectrum of vorLTsiR, a small reduction in intensity of both bands at 260 and 208 nm was observed (Fig. 2), suggesting that the characteristic A-form helix that is characteristic of siRNA in vorLTsiR was maintained. In the spectrum of spoLTsiR, however, the reduction in intensity of the band at 260 nm was more prominent with a drastic change in the large negative band at 208 nm to an acute signal at approximately 205 nm (Fig. 2). These results indicate that application of agitation caused less perturbation to the A-form helix of siRNA during lipoplex formation.

Table 2
Statistical evaluation and validation tests applied to the mathematical model.

Factor	SS	DF	MS	F
X_1 (lineal)	7433.87	1	7433.87	144.09*
X_1 (quadratic)	4.28	1	4.28	0.083
X_2 (lineal)	11,327.63	1	11,327.63	219.57*
X_2 (quadratic)	399.89	1	399.89	7.75*
X_3 (lineal)	8236.86	1	8236.86	159.66*
X_3 (quadratic)	19.86	1	19.86	0.39
X_1 *vs.* X_2 (interaction)	733.99	1	733.99	14.23*
X_1 *vs.* X_3 (interaction)	69.84	1	69.84	1.35
X_2 *vs.* X_3 (interaction)	2469.64	1	2469.64	47.87*
Lack of fit	1220.16	17	71.77	1.39
Pure error	4178.81	81	51.59	
Total	36,094.83	107		
R^2	0.85042			

X_1 = dose of siRNA (nM); X_2 = vortex speed (rpm); X_3 = vortex time (min); SS, sum of squares; DF, degrees of freedom; MS, mean square; F = test F (Fisher).
* Significant for $\alpha = 0.05$.

3.3. In vitro siRNA gene knockdown

Twenty-seven vorLTsiR were prepared by changing siRNA doses and vortex conditions (speed and time). *In vitro* luciferase gene knockdown effects by these vorLTsiRs were determined as described above (Table 1). The gene knockdown effect of prepared vorLTsiRs was strongly dependent on all 3 variables: the efficacy correlated with increases in siRNA, vortex speed and vortex time.

3.4. Statistical analysis to identify the most important variable in vorLTsiR-mediated gene knockdown

The *in vitro* gene knockdown data (Table 1) were applied to the generation of a second-order model for the dependent variable (Eqs. (1) and (2)). The regression analysis relating to *in vitro* gene knockdown data was carried out with Eq. (3) and a summary of the analysis is shown in Table 2. The gene silencing effect estimated from the model agreed well with the *in vitro* gene knockdown data (coefficient of determination [R^2] = 0.8504)

Table 3
Statistics for the regression coefficients and estimated effects.

Factor	Coefficient	SE	t-Test$_{(coeffic.)}$	Effect	t-Test$_{(effect)}$
Mean	67.08	1.829	36.69*	–	–
X_1 (lineal)	−10.16	0.846	−12.01*	−20.32	−12.01*
X_1 (quadratic)	0.42	1.466	0.29	−0.42	−0.29
X_2 (lineal)	−12.54	0.846	−14.82*	−25.09	−14.82*
X_2 (quadratic)	−2.04	0.733	−2.78*	4.08	2.78*
X_3 (lineal)	−10.70	0.846	−12.64*	−21.39	−12.64*
X_3 (quadratic)	0.91	1.466	0.62	−0.91	−0.62
X_1 *vs.* X_2 (interaction)	3.91	1.036	3.77*	7.82	3.77*
X_1 *vs.* X_3 (interaction)	−1.20	1.036	−1.16	−2.41	−1.16
X_2 *vs.* X_3 (interaction)	−7.17	1.036	−6.92*	−14.35	−6.92*

X_1 = dose of siRNA (nM); X_2 = vortex speed (rpm); X_3 = vortex time (min); SE, standard error.
* Significant for $\alpha = 0.05$.

(Table 2). An insignificant result for the lack of fit confirmed that the experimental variability is due mainly to the variables studied, and no violations of the model assumptions occurred (Wherle et al., 1995).

Considering the results for the statistical analysis by *t*-test, it was clear that the linear contributions of the factors showed important and quite similar effects (Table 3) and had a negative effect on the *in vitro* luciferase gene knockdown effect (Table 1). The contribution of the second-order term was interpreted as the presence of a curvature and represents the nature of the response surface system (maximum, minimum, or saddle system). The positive signal thus observed with the speed (quadratic) term revealed the convex form of the curve. However, only a slight influence could be imputed to this term when compared to linear terms. In the same way, the interactions between vortex speed and the other variables were also found to be statistically significant but they had just a minor importance in the response behavior (Table 3).

According to the *t*-test, non-significant terms of the model should be withdrawn. The model was recalculated and only the significant terms ($\alpha < 0.05$) were selected for the equation. The results obtained for the statistical validation of the model were presented in Table 4. Thus, the experimental behavior could be satisfactory described by Eq. (4):

Table 4
Statistical analysis of the simplified model.

Factor	Coefficient	t-Test$_{(coeffic.)}$	F-test$_{(ANOVA)}$
Mean	67.08	94.41*	–
X_1 (lineal)	−10.16	−12.00*	144.09*
X_2 (lineal)	−12.54	−14.82*	219.57*
X_2 (quadratic)	−2.04	2.78*	7.75*
X_3 (lineal)	−10.70	−12.64*	159.66*
X_1 *vs.* X_2 (interaction)	3.91	3.77*	14.23*
X_2 *vs.* X_3 (interaction)	−7.17	−6.92*	47.87*
Lack of fit	–	–	1.27
R_2	0.8478		

X_1 = dose of siRNA (nM); X_2 = vortex speed (rpm); X_3 = vortex time (min).
* Significant for $\alpha = 0.05$.

$$\text{RNAi effect (F-luc/R-luc)} = 67.08 - 10.16[X_1] - 10.69[X_3] + 3.91[X_1][X_2] - 7.17[X_2][X_3] + 0.42[X_1]^2 - 2.04[X_2]^2 \quad (4)$$

Validation experiments were carried out by ANOVA and multiple-correlation coefficient to verify the availability and the accuracy of

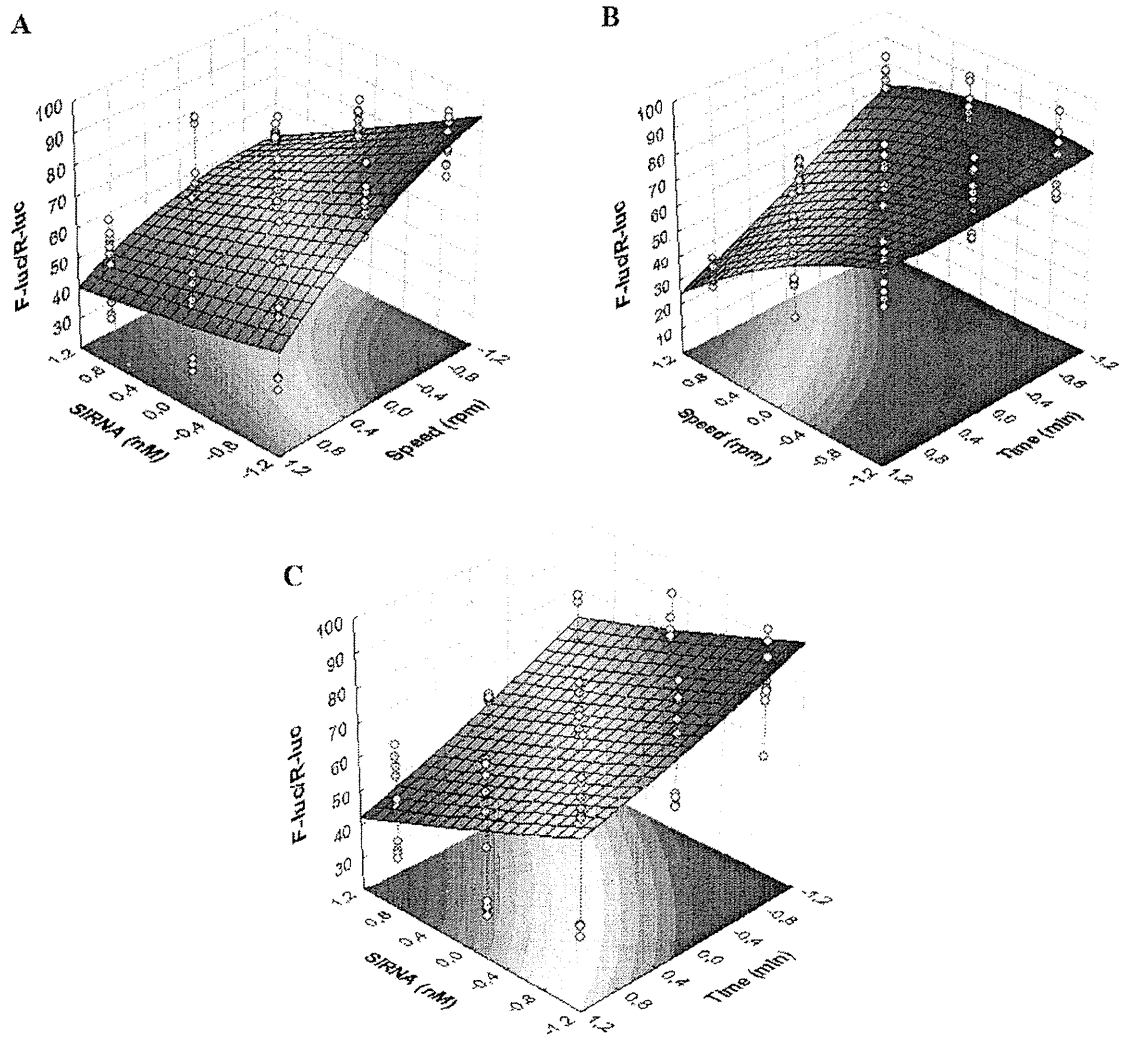

Fig. 3. Response surface plots showing the effect of siRNA dose and vortex speed (A), the effect of vortex speed and vortex time (B), and the effect of siRNA dose and vortex time (C) on the *in vitro* luciferase gene knockdown effect.

the models showed that the predict values agreed well with the experimental values (Table 4).

The estimated response surface plots of the effect of the variables on the *in vitro* luciferase gene knockdown effect are shown in Fig. 3. The response surface plots demonstrated that an increase in the siRNA dose expectedly results in an increase in the gene silencing effect. On the other hand, the plots demonstrated that an increase in the vortex speed promotes an efficient *in vitro* luciferase gene silencing effect at a lower siRNA dose. Concerning the association of the vortex speed and vortex time, the luciferase gene silencing effect is assumed to increase abruptly when both variables, *i.e.* vortex speed and vortex time, are at their highest level. This indicates that for vorLTsiR, vortex time contributes, to some extent, to vortex speed on the effective gene knockdown effect of siRNA. Nevertheless, it also assumes that an effective gene knockdown with the variable vortex time at a constant vortex speed is dependent on the siRNA dose. Under optimal conditions, *i.e.* 2500 rpm for 10 min, an induced luciferase gene knockdown could be achieved with a 4-fold lower siRNA dose (Fig. 3B). This estimation agreed well with the experimental data, as shown in Table 1. These results suggest that all 3 variables are significantly important, but statistically the vortex speed is the most important for the *in vitro* gene knockdown effect of vorLTsiR.

4. Discussion

Lipid molecules are known to interact with nucleic acids, either electrostatically *via* hydrophobic interaction or *via* hydrogen bonding (Lasic and Templeton, 1996). The FRET study (Fig. 1) indicated that in spoLTsiR, siRNA preferentially interacts with a cationic liposome through DC-6-14, while in vorLTsiR, siRNA preferentially interacts with a cationic liposome *via* DC-6-14 as well as DOPE. Our cationic liposome, LT, was composed of three lipids: the monocationic lipid DC-6-14, cholesterol, and DOPE. Cholesterol and DOPE are the most common helper lipids of the cationic liposomes that are used for lipofection (Ramezani et al., 2009). DOPE intensively affects the physicochemical properties of lipoplexes containing monocationic lipids such as *N*-(1-(2,3-dioleoyloxy)propyl)-*N*,*N*,*N*-trimethylammonium chloride (DOTAP) or 1,2-dimyristyloxypropyl-3-dimethyl-hydroxyethylammonium bromide (DMRIE) (Felgner et al., 1994; Zuidam and Barenholz, 1997). DOPE is zwitterionic at near neutral pH (Ellens et al., 1986; Siegel and Epand, 1997) and also contributes to lower the overall positive charge and surface potential of a cationic liposome through the formation of a salt bridge (ion pairing) between its phosphate group and the quaternary amine group on the monocationic lipid. The chemical structure of DC-6-14 closely resembles the chemical structure of DOTAP and DMRIE. It is very likely that the balance between the acyl chain (length, unsaturation) and headgroup moieties (charge, hydrophilicity) could modulate the interactions guiding the formation of a salt bridge between the phosphate group on DOPE and the quaternary amine group on DC-6-14 (Sugahara et al., 2002; Shaikh et al., 2004, 2006). In such a case, because DOPE would contribute to lower the overall positive charge in the membrane, the location and order of the positive charges in the membrane are not in a good distribution, and the surface potential of the LT therefore becomes entirely lowered. Accordingly, it is likely that, in spoLTsiR, the electrostatic association of siRNA to cationic charges in the LT occur disorderedly. On the other hand, in vorLTsiR, the constant and intense agitation by vortexing would function as a driving force to gain entropy separating the interactions between the cationic lipid DC-6-14 and DOPE, and thereby promoting interactions between these cationic lipids and siRNA (Zuidam and Barenholz, 1997; Zuidam et al., 1999). The dynamic environment created by vortexing seems to promote an interaction of siRNA with the surface of LT and, consequently, helps siRNA achieve a better distribution on it (Wang and MacDonald, 2004; Koynova et al., 2007), although this is one of factors to gain better gene knockdown effect by vorLTsiR.

siRNA is a small tri-dimensional nanometric rod with an average single-molecule size below 10 nm in length and approximately 2 nm in diameter (Kim et al., 2009). Since its anionic groups are disposed at the side of the molecule, they must interact laterally with positively charged lipids in the membrane of a cationic liposome (Spagnou et al., 2004). In a CD experiment, the lateral anionic groups of an siRNA molecule in the lipoplexes is expected to cause either of the 2 polarizations to absorb more, and this wavelength-dependent difference can yield an interaction of siRNA with a cationic liposome during the lipoplex preparation procedure. A CD study (Fig. 2) showed that the intensity of the characteristic bands of the A-form helix of siRNA was reduced following its interaction with cationic liposome. The reduction in intensity was more prominent in spoLTsiR than in vorLTsiR, which caused an important shift in the large negative band at 208 nm to an acute band near 205 nm.

Previous studies have shown that electrostatic interaction between cationic liposomes and nucleic acids causes each component to dehydrate during lipoplex formation (Zhang et al., 2003; Hirsch-Lerner and Barenholz, 1999). The dehydration of the polar head groups implies a reduction in the number of water molecules separating positive and negative charges after complexation (Lasic and Templeton, 1996; Hirsch-Lerner and Barenholz, 1999). It thus might be that the closer the molecules, the more efficient and strong must be the interaction between siRNA and cationic lipids in vorLTsiR. In addition, under such conditions, other forces, such as elastic (bending and stretching) and hydrogen bonding forces, could contribute to the complementary and harmonious association of siRNA and cationic liposomes (Chong and Sugar, 2002; Janas et al., 2006). Their harmonious association might result in the formation of smaller and homogeneous lipoplexes ($\leq$200 nm), loading a larger amount of siRNA (80% of the dose) (Barichello et al., 2011). However, the larger number of dehydrated polar head groups in spoLTsiR could indeed trigger a relatively uncontrolled interactive process between lipoplexes in the presence of counter ions (Opti-MEM), leading to lipoplexes of excessive size and poor stability (Barichello et al., 2011). Such differences in physicochemical properties between spoLTsiR and vorLTsiR might be a major cause in the shift of the entry pathway increasing the internalization of siRNA and resulting in the increased *in vitro* gene knockdown efficacy of vorLTsiR (Barichello et al., 2011).

The factorial design and response surface plots (Fig. 3) demonstrated that an increase in siRNA dose expectedly increased the gene knockdown effect. However, the plots also indicated that an increase in vortex speed achieved an efficient gene knockdown effect at a lower siRNA dose. In addition, the vortex time cooperatively contributed to the vortex speed, but at a constant vortex speed, the vortex time did not contribute. Collectively, it appears that among the variables we studied, vortex speed was the most important variable in achieving the highest gene knockdown effect by vorLTsiR. The higher energy transmission induced by agitation likely increased reorganization of the positively charged cationic lipids DC-6-14 and DOPE in the liposomal membrane to harmoniously accommodate the negatively charged siRNA on a cationic liposome.

5. Conclusion

The high energy transmitted by the application of agitation during lipoplex formation harmonized the interaction of siRNA with the positively charged lipids (DC-6-14 and DOPE) in cationic liposomes, resulting in a superior gene knockdown efficacy of vorLTsiR

compared with spoLTsiR. Our results indicate that control over the variables contributing to lipoplex formation is required in order to obtain reliable and reproducible siRNA-lipoplexes and a superior *in vitro* gene knockdown effect. The selection of the correct lipoplex preparation procedure will avoid drawbacks that could jeopardize the potential use of non-viral vectors for siRNA therapy.

Acknowledgements

The authors thank Mr. James L. McDonald for his helpful advice in developing the English manuscript. This work was supported in part by Grant-in-Aid for Scientific Research (B) (23390012), the Ministry of Education, Culture, Sports, Science and Technology, Japan, and the Health and Labour Sciences Research Grants for Research on Advanced Medical Technology from The Ministry of Health, Labour and Welfare of Japan. We thank the Japan Association for the Advancement of Medical Equipment for supporting a Postdoctoral Fellowship for Dr. Jose Mario Barichello.

References

Barichello, J.M., Kizuki, S., Tagami, T., Asai, T., Ishida, T., Kikuchi, H., Oku, N., Kiwada, H., 2011. Agitation during lipoplex formation improves the gene knockdown effect of siRNA. Int. J. Pharm. 410, 153–160.

Chong, P.L., Sugar, I.P., 2002. Fluorescence studies of lipid regular distribution in membranes. Chem. Phys. Lipids 116, 153–175.

Dillen, K., Vandervoort, J., Van den Mooter, G., Verheyden, L., Ludwig, A., 2004. Factorial design, physicochemical characterisation and activity of ciprofloxacin-PLGA nanoparticles. Int. J. Pharm. 275, 171–187.

Elbashir, S.M., Harborth, J., Lendeckel, W., Yalcin, A., Weber, K., Tuschl, T., 2001. Duplexes of 21-nucleotide RNAs mediate RNA interference in cultured mammalian cells. Nature 411, 494–498.

Ellens, H., Bentz, J., Szoka, F., 1986. Destabilization of phosphatidylethanolamine liposomes at the hexagonal phase transition temperature. Biochemistry 25, 285–294.

Felgner, J.H., Kumar, R., Sridhar, C.N., Wheeler, C.J., Tsai, Y.J., Border, R., Ramsey, P., Martin, M., Felgner, P.L., 1994. Enhanced gene delivery and mechanism studies with a novel series of cationic lipid formulations. J. Biol. Chem. 269, 2550–2561.

Gonzalez-Rodriguez, M.L., Barros, L.B., Palma, J., Gonzalez-Rodriguez, P.L., Rabasco, A.M., 2007. Application of statistical experimental design to study the formulation variables influencing the coating process of lidocaine liposomes. Int. J. Pharm. 337, 336–345.

Hirsch-Lerner, D., Barenholz, Y., 1999. Hydration of lipoplexes commonly used in gene delivery: follow-up by laurdan fluorescence changes and quantification by differential scanning calorimetry. Biochim. Biophys. Acta 1461, 47–57.

Janas, T., Janas, T., Yarus, M., 2006. Specific RNA binding to ordered phospholipid bilayers. Nucleic Acids Res. 34, 2128–2136.

Kim, S., Garg, H., Joshi, A., Manjunath, N., 2009. Strategies for targeted nonviral delivery of siRNAs in vivo. Trends Mol. Med. 15, 491–500.

Koynova, R., Tarahovsky, Y.S., Wang, L., MacDonald, R.C., 2007. Lipoplex formulation of superior efficacy exhibits high surface activity and fusogenicity, and readily releases DNA. Biochim. Biophys. Acta 1768, 375–386.

Lasic, D.D., Templeton, N.S., 1996. Liposomes in gene delivery. Adv. Drug Deliv. Rev. 20, 221–266.

Li, C.X., Parker, A., Menocal, E., Xiang, S., Borodyansky, L., Fruehauf, J.H., 2006. Delivery of RNA interference. Cell Cycle 5, 2103–2109.

Li, W., Ishida, T., Tachibana, R., Almofti, M.R., Wang, X., Kiwada, H., 2004. Cell type-specific gene expression, mediated by TFL-3, a cationic liposomal vector, is controlled by a post-transcription process of delivered plasmid DNA. Int. J. Pharm. 276, 67–74.

Lima, M.C.P., Simoes, S., Pires, P., Faneca, H., Duzgunes, N., 2001. Cationic lipid-DNA complexes in gene delivery: from biophysics to biological applications. Adv. Drug Deliv. Rev. 47, 277–294.

Ramezani, M., Khoshhamdam, M., Dehshahri, A., Malaekeh-Nikouei, B., 2009. The influence of size, lipid composition and bilayer fluidity of cationic liposomes on the transfection efficiency of nanolipoplexes. Colloids Surf. B: Biointerfaces 72, 1–5.

Shaikh, S.R., Dumaual, A.C., Castillo, A., LoCascio, D., Siddiqui, R.A., Stillwell, W., Wassall, S.R., 2004. Oleic and Docosahexaenoic acid differentially phase separate from lipid raft molecules: a comparative NMR, DSC, AFM, and detergent extraction study. Biophys. J. 87, 1752–1766.

Shaikh, S.R., Cherezov, V., Caffrey, M., Soni, S.P., LoCascio, D., Stillwell, W., Wassall, S.R., 2006. Molecular organization of cholesterol in unsaturated phophatidylethanolamines: X-ray diffraction and solid state ^{2}H NMR reveal differences with phosphatidylcholines. J. Am. Chem. Soc. 128, 5375–5383.

Siegel, D., Epand, R., 1997. The mechanism of lamellar-to-inverted hexagonal phase transitions in phosphatidylethanolamine: implications for membrane fusion mechanism. Biophys. J. 73, 3089–3111.

Spagnou, S., Miller, A., Keller, M., 2004. Lipidic carriers of siRNA: differences in the formulation, cellular uptake, and delivery with plasmid DNA. Biochemistry 43, 13348–13356.

Sugahara, M., Uragami, M., Regen, S.L., 2002. Selective sterol–phospholipid associations in fluid bilayers. J. Am. Chem. Soc. 124, 4253–4256.

Wang, L., MacDonald, R.C., 2004. New strategy for transfection: mixtures of medium-chain and long-chain cationic lipids synergistically enhance transfection. Gene Ther. 11, 1358–1362.

Wherle, P., Magenheim, B., Benita, S., 1995. The influence of process parameters on the PLA nanoparticle size distribution, evaluation by means of factorial design. Eur. J. Pharm. Biopharm. 41, 19–26.

Xu, Y., Zhang, H., Thormeyer, D., Larsson, O., Du, Q., Elmen, J., Wahlestedt, C., Liang, Z., 2003. Effective small interfering RNAs and phosphorothioate antisense DNAs have different preferences for target sites in the luciferase mRNAs. Biochem. Biophys. Res. Commun. 306, 712–717.

Zelphati, O., Szoka Jr., F.C., 1996. Mechanism of oligonucleotide release from cationic liposomes. Proc. Natl. Acad. Sci. U.S.A. 93, 11493–11498.

Zhang, Y., Garzon-Rodriguez, W., Manning, M.C., Anchordoquy, T.J., 2003. The use of fluorescence resonance energy transfer to monitor dynamic changes of lipid–DNA interactions during lipoplex formation. Biochim. Biophys. Acta 1614, 182–192.

Zuidam, N.J., Barenholz, Y., 1997. Electrostatic parameters of cationic liposomes commonly used for gene delivery as determined by 4-heptadecyl-7-hydroxycoumarin. Biochim. Biophys. Acta 1329, 211–222.

Zuidam, N.J., Hirsch-Lerner, D., Margulies, S., Barenholz, Y., 1999. Lamellarity of cationic liposomes and mode of preparation of lipoplexes affect transfection efficiency. Biochim. Biophys. Acta 1419, 207–220.